

# Detecting and Locating Short-Circuit Faults in Electrical Mesh Networks

Nianga-Apila<sup>ORCID</sup>, Mathurin Gogom, Anedi Oko Ganongo<sup>ORCID</sup>, Rodolphe Gomba, Gilbert Ganga

Laboratoire de Génie Électrique et Électronique, École Nationale Supérieure Polytechnique (ENSP), Université Marien Nguabi, Brazzaville, République du Congo  
E-mail: apilanianga@gmail.com

**How to cite this paper:** Nianga-Apila, Gogom, M., Ganongo, A.O., Gomba, R. and Ganga, G. (2025) Detecting and Locating Short-Circuit Faults in Electrical Mesh Networks. *Energy and Power Engineering*, 17, 134-153. <https://doi.org/10.4236/epe.2025.176007>

**Received:** May 5, 2025

**Accepted:** June 24, 2025

**Published:** June 27, 2025

Copyright © 2025 by author(s) and Scientific Research Publishing Inc. This work is licensed under the Creative Commons Attribution International License (CC BY 4.0). <http://creativecommons.org/licenses/by/4.0/>



Open Access

## Abstract

This paper presents a method for detecting, classifying, and locating short-circuit faults in meshed electrical networks using Artificial Neural Networks (ANNs). The proposed approach is applied to a simulated 220 kV Congolese transmission line model developed in MATLAB/SIMULINK. The system uses voltage and current data as input, which are preprocessed through normalization, and is trained using a supervised backpropagation algorithm within a multilayer perceptron architecture. Designed for developing countries, where real-time fault visualization is often limited by the absence of dispatching centers and budgetary constraints, this solution offers a low-cost, autonomous alternative. It can integrate fault localization technologies, such as GPS or fiber optics. The results demonstrate high accuracy, with a mean square error of  $2.3001e-17$  for fault detection and  $3.5313e-18$  for fault classification and localization.

## Keywords

Meshed Electrical Networks, Short-Circuit Faults, Fault Localization, Artificial Intelligence, Artificial Neural Networks (ANNs), Fault Detection and Classification

## 1. Introduction

Electricity networks are designed, built and operated to ensure the transit of electrical energy and to withstand atmospheric conditions (wind, sun and rain), mechanical stresses and electrical overloads. Despite all the regulatory measures taken, electricity networks remain exposed to various disturbances (voltage drop, voltage imbalance, overvoltage, lack of synchronism and short circuits) [1]-[3]. When an electricity network is faced with overcurrents or voltage drops, the quick-

est solutions are to use traditional or modern compensators [4].

Voltage imbalance, which is common in medium and low voltage, is generally resolved by conventional or intelligent techniques [4]-[6]. Lack of synchronism is reduced by regulating the speed of rotating machinery [7] [8]. Furthermore, despite the protective devices installed to automatically isolate the affected areas, short circuits require rapid and accurate detection, classification and location to enable response teams to act promptly. This ability to react minimises the socio-economic damage that usually accompanies such incidents. This need is particularly critical in the electricity networks of developing countries, which do not have sophisticated dispatching centres for real-time monitoring [9]. These events can lead to blackouts, with major technical and economic consequences. The quicker you can locate an event, the more effective it is at restoring service. Conventional fault location methods, such as impedance-based approaches [10]-[12], genetic algorithms, travelling waves [13] [14] or neuro-fuzzy techniques [15] [16], have shown variable performance depending on the network conditions. In comparison, artificial neural networks (ANNs), although they have already been applied to this issue [17]-[20], offer significant advantages in terms of their ability to model complex relationships, generalise from noisy data, and adapt to the local specificities of real networks.

With this in mind, our work proposes an optimised ANN architecture for detecting, classifying and locating faults on transmission lines. The originality of our approach lies not only in the application to a simulated real network in Congo, but also in the integration of robust pre-processing including data normalisation (min-max method) and the addition of Gaussian noise to test the resilience of the model. Unlike traditional methods, our multilayer back-propagation network is able to provide accurate results from local data, without the need for an advanced communications infrastructure.

This study is based on data from 45 realistic scenarios simulated in MATLAB/SIMULINK, covering a wide range of faults and positions on the line. The proposed algorithm demonstrates remarkable efficiency, validated by low performance metrics (MSE), and thus responds to a concrete problem with an economically viable and technically efficient approach.

## 2. Theoretical Approach

### 2.1. Short Circuits

#### 2.1.1. Definition

A short-circuit is accidental or intentional contact between two points on an electrical circuit between which there is a potential difference. This causes a sudden increase in current, leading to high temperatures and the risk of fire.

#### 2.1.2. Causes or Origins

Short circuits can occur due to a variety of factors such as faulty wiring, damaged components or poor electrical installation. It is vital to take steps to prevent short circuits, including ensuring that electrical wiring is correctly installed and using protective devices such as fuses or circuit breakers. In the event of a short circuit,

it is imperative to act quickly to avoid any potential damage by isolating the infected part and then calling in professionals to repair the problem. These types of fault apply to all meshed or radial networks [2] [21].

### 2.1.3. Different Types of Short Circuit

There are different types of short circuit [2] [21].

### 2.1.4. Methods for Calculating Short-Circuit Current

To determine short-circuit currents, it is necessary to calculate the impedance of the circuit through which the current flows. The impedance is calculated by combining the resistances and reactances of the fault loop, from the circuit's power source to the point of interest or point under consideration.

- Isolated single-phase short-circuit: It corresponds to a fault between one phase and the neutral, supplied at a single voltage ( $V = U/3$ ).  $I_{cc1}$  debited is then [2] [21].

$$I_{cc} = \frac{U}{\sqrt{3}(Z_{cc} + Z_{ln})} \quad (1)$$

- Isolated two-phase short-circuit: It corresponds to a fault between two phases, supplied with a phase-to-phase voltage  $U$ . The short-circuit current is [2] [21]:

$$I_{cc} = \frac{U}{2Z_{cc}} \quad (2)$$

- Three-phase short-circuit: This is the fault which corresponds to the combination of the three phases. The short-circuit current is [2] [21]:

$$I_{cc} = \frac{U}{Z_{cc}\sqrt{3}} \quad (3)$$

With is  $Z_{cc}$  :

$$Z_{cc} = \sqrt{\sum R^2 + \sum X^2} \quad (4)$$

These different types of short circuit must be detected, classified and located.

## 2.2. Detecting, Classifying and Locating Short Circuits

### 2.2.1. Detecting

Fault detection involves identifying that a short-circuit has occurred in the meshed electrical network by analysing abnormal variations in the currents and voltages measured.

### 2.2.2. Classification

Fault classification makes it possible to determine the type of short-circuit (three-phase, two-phase, single-phase, etc.) that has occurred in the meshed network using the symmetrical components of the currents and voltages.

### 2.2.3. Location

The aim of fault location is to identify the zone or section of the meshed network where the short-circuit occurred, using measurements taken at the various nodes

and accurately modelling the network topology.

### 2.3. Artificial Neural Networks

Artificial neural networks (ANNs) are architectures inspired by the neuronal cells of the human brain, organised in interconnected layers. A feedforward artificial neural network, such as a perceptron, uses mathematical models of neurons that are simpler than biological models. These networks are designed to perform specific tasks using interconnected processing elements. The behaviour of an artificial neuron comprises two phases: the pre-processing of the data by a weighted sum of the inputs, which is calculated according to the following expression:

$$x_1\omega_1 + x_2\omega_2 + x_3\omega_3 + \dots + x_n\omega_n = \sum_{k=1}^n x_k\omega_k \quad (5)$$

In addition, there is a threshold  $b\omega_0$

$$S = \sum_{k=1}^n x_k\omega_k + b\omega_0 \quad (6)$$

The result is then transformed by a non-linear activation function (sometimes called an output function),  $f(S)$ . A transfer function then calculates the neuron's internal state, influencing the output. Different types of activation function, such as the sigmoid, determine the impact of inputs on the output. The basic operation of ANNs is to find the relationship between input and target data by adjusting the weights to optimise performance.

ANNs initialise the values of  $W$ , calculate the error between the outputs and the targets, then adjust the values of  $W$  until a suitable MSE is reached. This method is called error backpropagation, which allows ANN to improve by correcting errors. Backpropagation of errors, also known as back propagation (BP), is an algorithm used in the field of machine learning for training artificial neural networks. It is a supervised algorithm whose objective is to adjust the weights of the PCM network so as to minimise a differentiable cost function, such as the squared error between the output of the network and the desired output:

$$E(n) = \|d(n) - x_L(n)\|^2 \quad (7)$$

where  $x_L(n)$  is the network output at time  $n$  and  $d(n)$  is the desired output. The BP algorithm descends the gradient on the error criterion to reach the minimum. The gradient of  $E(n)$  is calculated for all weights as follows:

$$\frac{\partial E(n)}{\partial w_{ijk}(n)} = \frac{\partial E(n)}{\partial y_{ik}(n)} \cdot \frac{\partial y_{ik}(n)}{\partial w_{ijk}(n)} = \frac{\partial E(n)}{\partial y_{ik}(n)} \cdot x_{i-1j} \quad (8)$$

In the case of the output layer ( $i = L$ ), the output error term  $\delta_{Lk}$  is evaluated as follows:

$$\delta_{Lk} = \frac{\partial E(n)}{\partial y_{ik}(n)} = 2f'(\partial y_{ik})(d_k - x_{ik}) \quad (9)$$

where  $f'$ : is the derivative of the activation function:

$$f'(x) = \frac{df(x)}{dx} \tag{10}$$

For hidden layers, the  $\delta_{ik}$  error term of neuron ( $i, k$ ) is given by:

$$\delta_{ik} = 2f'(\partial y_{ik}) \sum_{j=1}^{N(i+1)} \delta_{i+1j} W_{i+1jk} \tag{11}$$

The modification of weights and biases is obtained according to the following equations:

$$\begin{aligned} w_{ijk}(n+1) &= w_{ijk}(n) + \mu \delta_{ik} \cdot x_{i-1j} + \alpha (w_{ijk}(n) - w_{ijk}(n-1)) \\ &= b_{ijk}(n) + \mu \delta_{ik} \end{aligned} \tag{12}$$

where  $\mu$  is the learning step and  $\alpha$  the inertia term (Momentum). The choice of learning step has a major influence on the speed of convergence: too small a step slows down learning, while too large a step creates a risk of instability. It is even possible for the algorithm to encounter a local minimum. The inertia term (Momentum  $0 < \alpha < 1.0$ ) enables the algorithm to escape from the local minimum and limit oscillations during training, by taking into account changes in the previous stages and therefore converging more quickly.

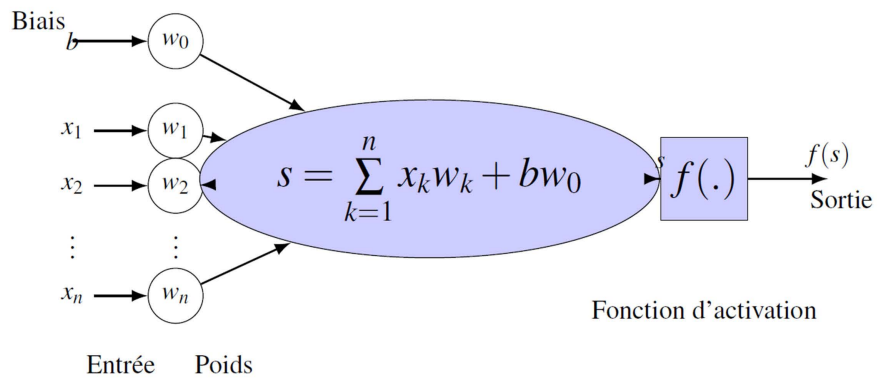


**Figure 1.** Architecture of the ANN.

**2.3.1. Detecting**

**Figure 1** model is used to simulate 11 types of fault (A-G; B-G; C-G; A-B-G; A-C-G; B-C-G; A-B; A-C; B-C; A-B-C; A-B-C-G). The network structure comprises an input layer of 8 neurons, a hidden layer of 10 neurons and an output layer of 1 neuron. The structure of the neural network chosen for fault detection is shown in **Figure 2**.

**Figure 3(a)** shows the training performance of the neural network. The learning performance in terms of squared error of the neural network for the three learning stages (Training, Validation and Testing). It can be noted that after the decrease in the mean squared error (MSE) achieved at the end of the learning process, the best performance of the (MSE) for the validation stage by this neural network is 2.3001e-17 after 13 iterations. **Figure 3(b)** represents the best fitted linear regression between the desired and desired outputs for the three learning stages (Training, Testing and Validation) of the neural network in **Figure 2**.

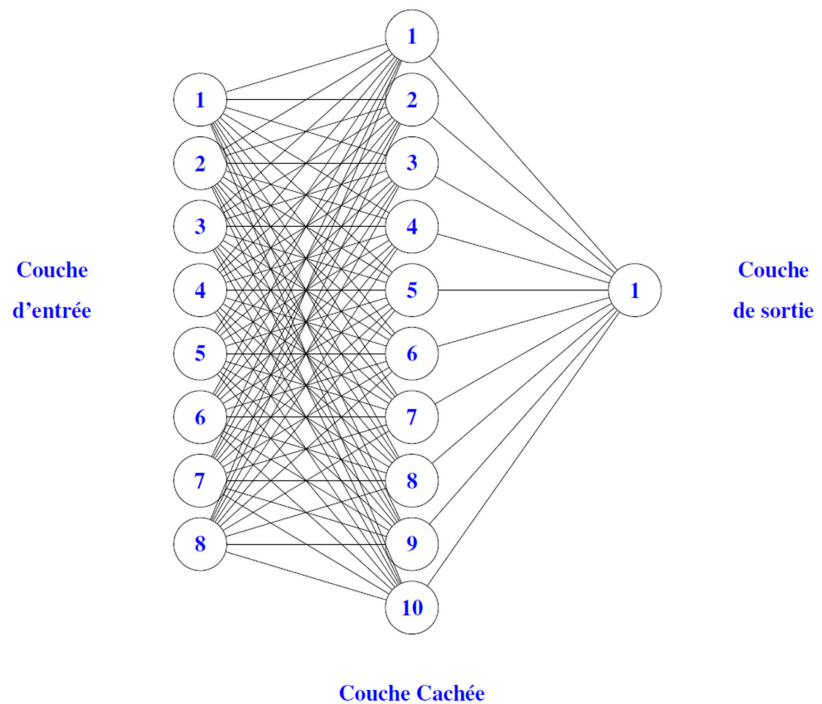


Figure 2. RNA for fault detection.

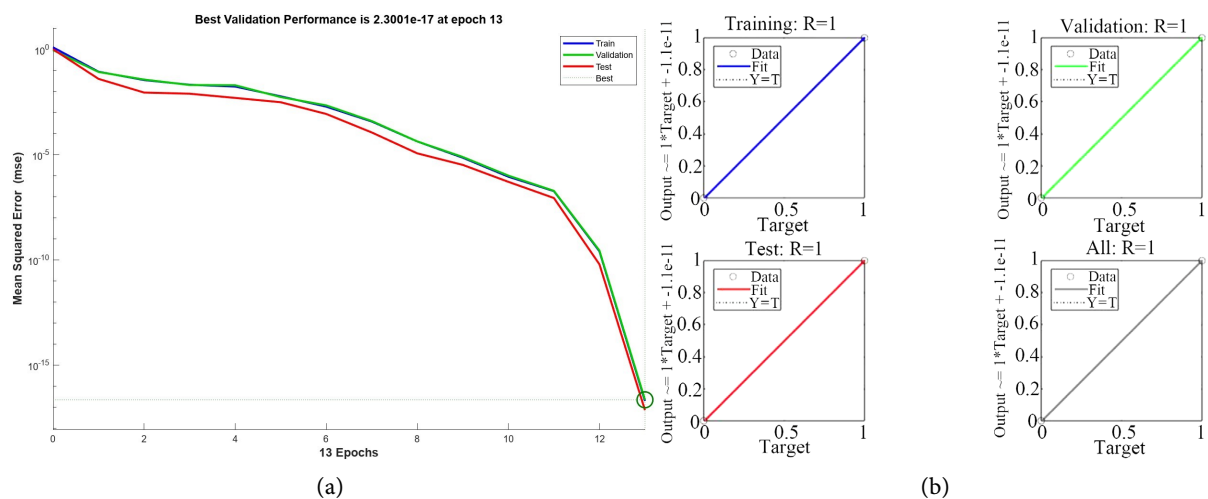


Figure 3. The learning performance for detection. (a) Squared error performance for detection; (b) Regression adjustment of detection results.

Table A1 in Annexe6 illustrates the generalisation capability of the Artificial Neural Network (ANN) for short circuit detection. For example, in the event of a single-phase fault, the expected output is 1, but the ANN provides a value of 0.99. The error, calculated as the difference between the desired output and that obtained, is then expressed as a percentage. This evaluation is applied to all cases, with or without a fault, in order to check the overall reliability of the model.

### 2.3.2. Classification and Localisation

Once a fault is detected on a power line, the next step is to classify the type of fault

and locate its location in the network. The process of designing and developing neural classifiers and locators is similar to the previous section. The network output is 0 or 1, indicating whether there is a fault on the corresponding line (A, B, C or G, where A, B and C represent the three phases of the transmission line and G represents ground). The artificial neural network used has a three-layer structure: the input layer has 8 neurons, representing the voltage and current modules with each neuron in the hidden layer receiving a weighted linear combination of the inputs

$$Z_j^{(1)} = \sum_{i=1}^8 w_{ij}^{(1)} \cdot x_i + b_j^{(1)} \text{ pour } j = 1, \dots, 10 \tag{13}$$

Then we apply the activation function:

$$a_j^{(1)} = f\left(Z_j^{(1)}\right) \tag{14}$$

So we obtain a vector of 10 activations at the output of the hidden layer.

$$Z_k^{(2)} = \sum_{j=1}^{10} w_{jk}^{(2)} \cdot a_j + b_k^{(2)} \text{ pour } k = 1, \dots, 5 \tag{15}$$

And we apply the activation function again:

$$a_k^{(2)} = f\left(Z_k^{(2)}\right) \tag{16}$$

The output layer consists of five neurons: four for linear outputs and one dedicated to localization, as shown in **Figure 4**.

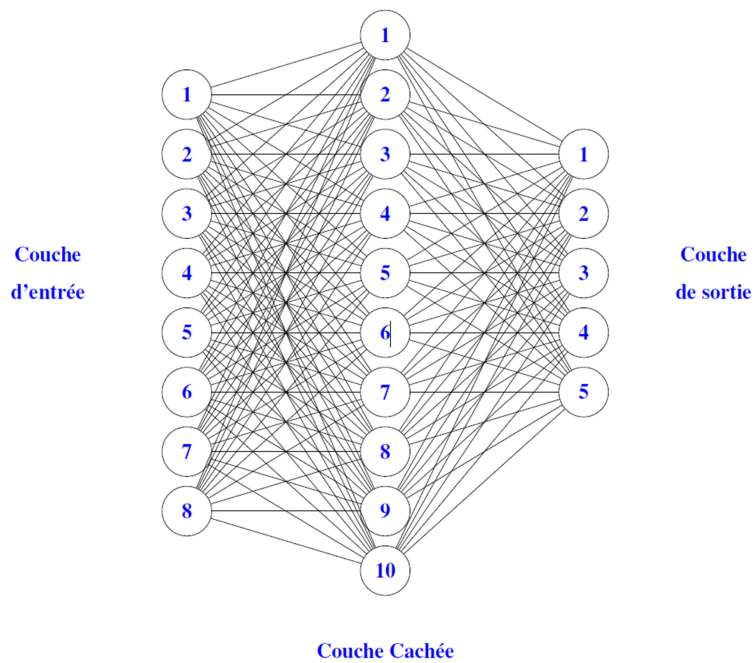


**Figure 4.** RNA architecture for classification.

The learning performance in terms of squared error of **Figure 5** neural network for the three learning stages (training, validation and test). It can be seen that after the reduction in mean square error (MSE) achieved at the end of the learning

process, the best execution of (MSE) for the validation stage by this neural network is  $3.5313e-18$  after 20 iterations.

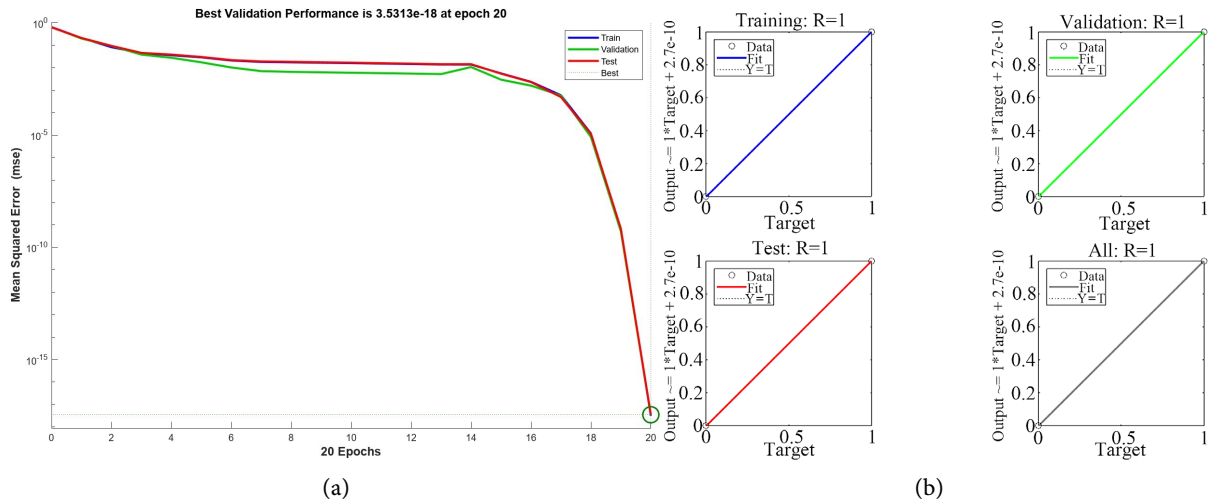


**Figure 5.** The learning performance for classification. (a) Squared error classification performance; (b) Regression adjustment of classification results.

**Table A2** in **Annexes A** shows the results of the generalisation test for the artificial neural network (ANN) used to classify short circuits. This evaluation method is applied to all types of fault in order to assess the accuracy of the model in recognising the different classes of short-circuit.

### 3. Electrical System Considered

The proposed transmission line is 220 kV and over 100 km long. It includes two voltage sources, one of 300 MW and the other of 50 MW. The transformer specifications are presented in **Table A3**, those of the load in **Table A4**, and those of the line in **Table A5**, in **Annexes B**.

**Figure 6** illustrates the studied power system, on which all simulations have been conducted. This model serves as the reference network for evaluating the fault detection and localization method.

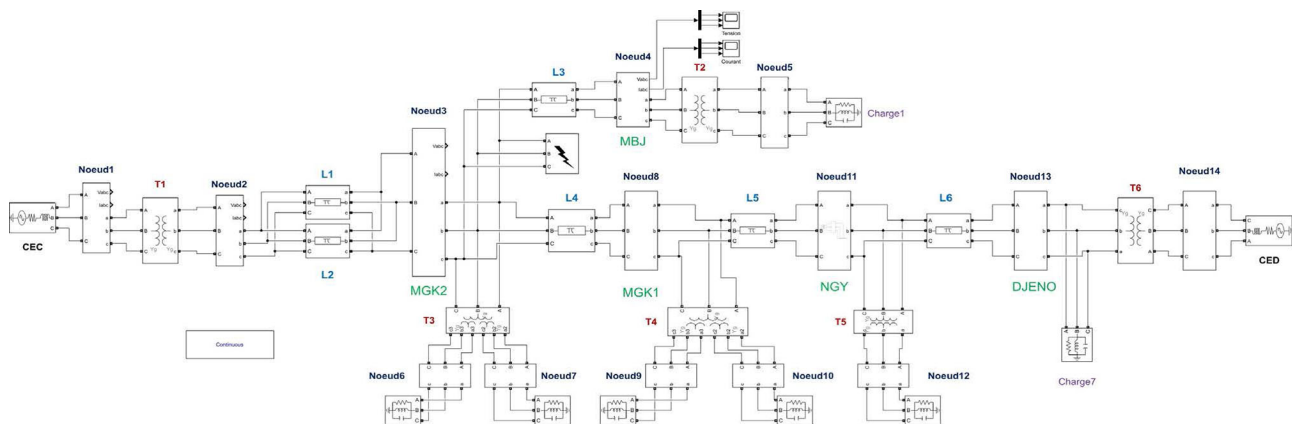


**Figure 6.** The system studied.

### 3.1. Fault Location System

Figure 7 presents the functional diagram of the proposed system, detailing the signal acquisition, preprocessing, and fault classification stages based on the neural network architecture.

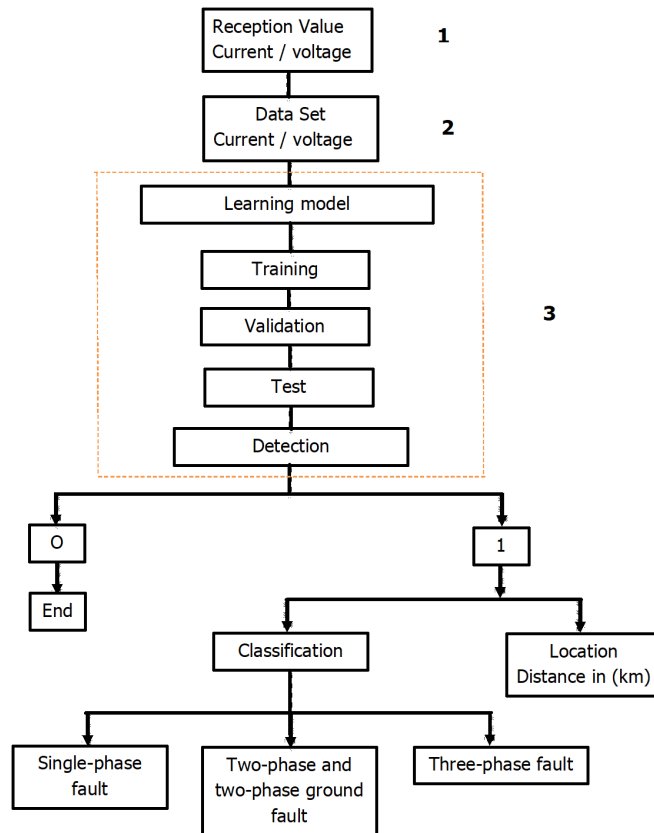


Figure 7. Functional diagram of the proposed system.

#### 3.1.1. Receiving Data

Taking values into account represents the essential basis of the fault detection process, ensuring that crucial data is collected rigorously and reliably. By focusing on voltage and current measurements, this stage enables the data to be prepared in the best possible way for subsequent stages, in particular by ensuring consistency in the structure of the dataset. Key aspects include real-time data collection, consistency checking and frictionless data transfer to the analysis system.

#### 3.1.2. Data-Set

Creating a dataset represents a crucial step in structuring and organizing the data required for a high-performing model. This section explores how raw voltage and current data are transformed into an exploitable and consistent format. Emphasis is placed on the integration of normalized and pre-processed values, thus ensuring the reliability and homogeneity of the dataset. By adopting a rigorous methodology, this step lays the foundation for optimal machine learning. Data is collected from healthy electrical networks as well as networks with short-circuits. These

data, representing different types of short-circuits, are gathered from simulations or online measurements. The data are then pre-processed to normalize values and eliminate noise, making them compatible with the neural network model.

**Data normalisation:** In order to ensure that the neural network is trained efficiently and to avoid any numerical dominance between the different input variables (voltages and currents), a Min-Max normalisation was applied to all the data. This method transforms each variable  $x$  according to the following formula:

$$x_{\text{norm}} = \frac{x - x_{\min}}{x_{\max} - x_{\min}} \quad (17)$$

or  $x_{\min}$  and  $x_{\max}$  represent the minimum and maximum values of the variable in question, respectively, with  $x$  represents an unnormalised raw value of an input variable to the neural network. This operation brings all the inputs into the range  $[0, 1]$ , guaranteeing faster convergence of the learning process and better numerical stability.

**Simulation of random noise:** To test the robustness of the model in conditions close to the real world, random Gaussian noise was added to the simulated voltage and current signals. These disturbances are intended to simulate the interference and inaccuracies inherent in measurements in a real electrical network. Several levels of noise (low, moderate, high) were tested, and the model demonstrated reliable detection, classification and localisation, even in the presence of noisy signals. This approach reinforces the experimental validity of the proposed solution.

### 3.1.3. ANN Algorithm

After normalization, these data are divided into training and testing sets to train the artificial neural network to learn how to distinguish between the two. Next, define the architecture of the neural network by choosing the number of layers and neurons, while selecting the appropriate activation function. Then, use the training data to adjust the weights of the neural network. Apply the backpropagation algorithm to minimize prediction error. Evaluate the model's performance using the test data. Calculate the Mean Squared Error (MSE) to measure the accuracy of the diagnosis. Apply the trained model to diagnose the presence of short-circuits in high-voltage electrical networks. When new data are presented to the neural network, it analyzes them and determines whether a short-circuit is present. If a short-circuit is detected, the neural network classifies it according to its type or nature and also localizes the point where the short-circuit occurs.

## 4. Simulations and Results

In order to assess the robustness of the proposed algorithm, a variety of realistic fault scenarios were simulated, covering the full range of short-circuit configurations likely to occur in a three-phase network. Simulated short circuit configurations include:

- Single-phase to ground: A-G; B-G; C-G

- Two-phase: A-B; A-C; B-C
- Two-phase ground: A-B-G; A-C-G; B-C-G
- Three-phase: A-B-C
- Three-phase to ground: A-B-C-G

The phases are defined as follows: A (phase 1), B (phase 2), C (phase 3), and G (ground). In order to build up a diverse and usable database, each of the eleven types of fault identified was simulated at different locations along the transmission line. A no-fault scenario was also included, bringing the total number of situations studied to forty-five. This data was then used to train, validate and test the neural network model.

For each scenario, current and voltage signals were collected at a sampling rate of 1 millisecond, over an observation window of 100 milliseconds. This is equivalent to 100 samples per signal. Given that three phases are involved, and that two quantities (voltage and current) are measured per phase, each case generates 600 values (3 phases  $\times$  2 measurements  $\times$  100 points), constituting a rich set for learning. The data collected was divided into three sub-sets according to a classic scheme: 70% was used for learning, 15% for validation and 15% for testing. This division is designed to guarantee the reliability of the model evaluation while avoiding overlearning.

For the simulations of the network in **Figure 6** with a fault, we have placed a block of the different types of short-circuit on line 3 - 4, and we are going to focus on these cases:

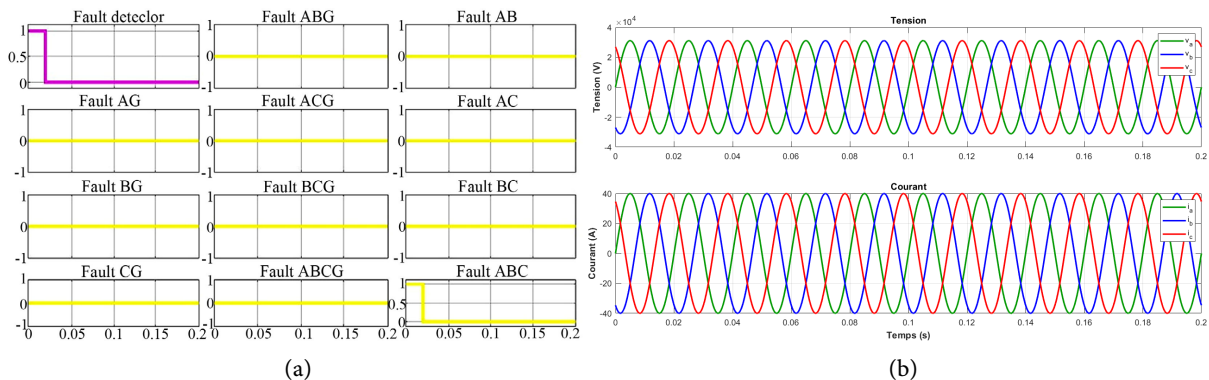


**Figure 8.** Diagnosis indicating no type of fault. (a) No faults on any phase; (b) Current and voltage curve showing no fault.

After simulating **Figure 6** network, we can see that **Figure 8(a)** and **Figure 8(b)** show us that the neural network was able to detect the presence of no short-circuit on line 3 - 4. Then, in the second block, we have two other blocks displaying the results. In the classification, we also find the figures zero in the first, second and third phases, as well as in the earth, and also zero in the last block, which gives the location of the fault, giving its exact distance (see **Figure S2(a)**, in **Annexes C**).

**Figure 9(a)** and **Figure 9(b)** show us that the neural network was able to detect the presence of a short-circuit on line 3 - 4, the short-circuit is of the single-phase type between phase A and earth node G, on the block, the first 1 marks a fault on phase A and the last is earth node G and this short-circuit occurred at a distance of 4.72 km from node 1 (see **Figure S2(b)**, in **Annexes C**).

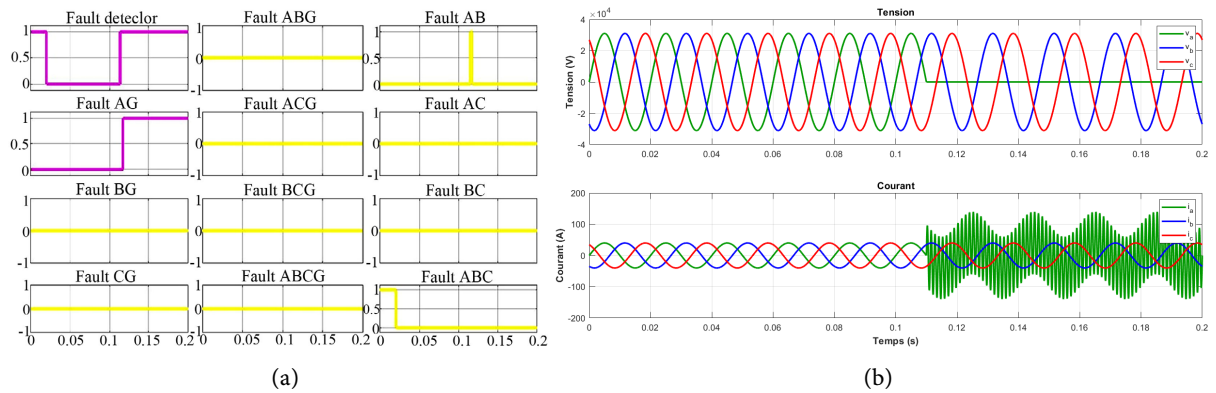


**Figure 9.** Diagnosis of a single-phase fault. (a) Fault between phase A and earth G; (b) voltage and current curve with a single-phase fault.

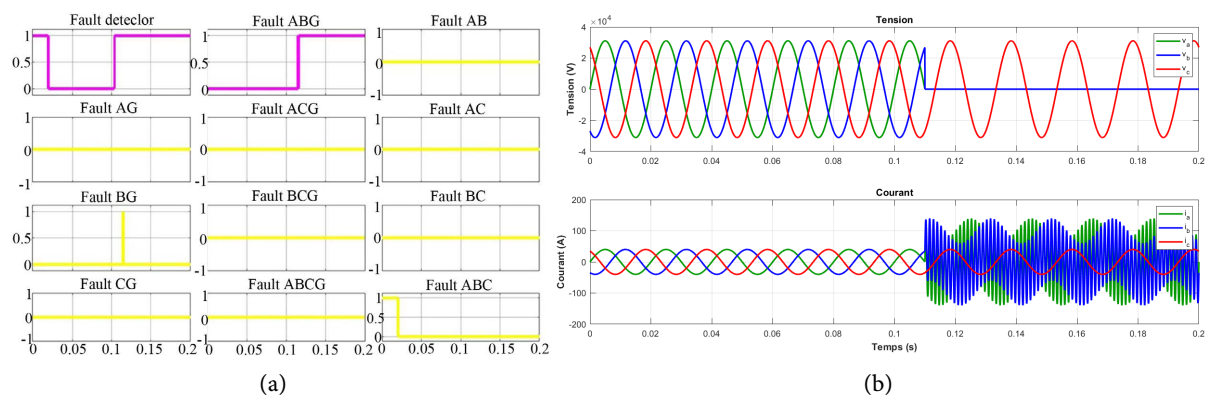


**Figure 10.** Diagnosis of a two-phase fault. (a) Fault between A, B et G; (b) voltage and current curve with a two-phase fault.

**Figure 10(a)** and **Figure 10(b)** show us that the neural network was able to detect the presence of a short-circuit of the two-phase/earth type at the level of line 3 - 4, and this occurred between phase A, phase B and earth (G), on the display the first 1 marks a fault on phase A, the second on phase B and the last is earth node G and this short-circuit occurred at a distance of 5.19 km from node 1 (see **Figure S2(d)**, in **Annexes C**).

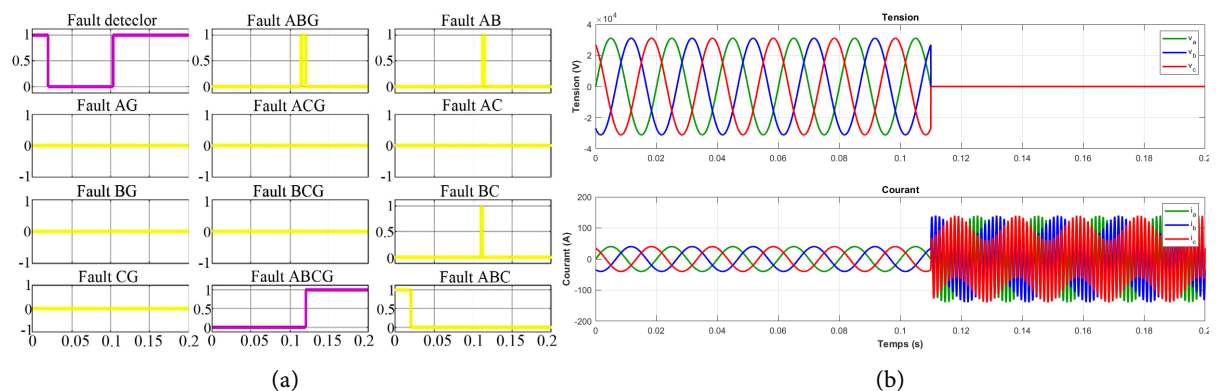


**Figure 11.** Diagnosis of a three-phase fault. (a) Fault between A, B, C and G; (b) voltage and current curve with a three-phase fault.

**Figure 11(a)** and **Figure 11(b)** show us that the neural network was able to detect the presence of a short-circuit of the three-phase-earth type on line 3 - 4, and this occurred between phase A, phase B, phase C and ground point G, on the display the first 1 marks a fault on phase A, the second on phase B, the third on phase C and the last is earth node G and this short-circuit occurred at a distance of 5.17 km from node 1 (see **Figure S2(d)** in **Annexes C**).

## 5. Conclusions

The detection and localization of short circuits in meshed electrical networks play a crucial role in maintaining the stability and security of energy infrastructures. The integration of artificial neural networks (ANN) provides an optimized and systematic approach, enhancing anomaly identification and fault management. Leveraging machine learning principles, these models accurately recognize disturbances while systematically categorizing them, thereby facilitating the implementation of appropriate corrective measures.

To evaluate the effectiveness of the developed system, the Mean Squared Error (MSE) was used as a quantitative performance indicator. The obtained results reveal a remarkable ability to detect and classify faults: after 13 iterations, an MSE of  $2.3001e-17$  was recorded for the detection phase, while an MSE of  $3.5313e-18$  was achieved after 20 iterations for the classification and localization of anomalies. These values demonstrate the model's consistency and the reliability of its approach in disturbance analysis. Experiments confirmed extremely low error margins, proving the system's ability to precisely locate faults. This observation highlights the value of a preventive approach in electrical network management, where rapid detection and efficient intervention help reduce the risk of equipment degradation and ensure service continuity.

The integration of these advanced analytical tools represents a significant advancement for power grid operators. In addition to improving power supply management, these technologies enhance safety standards for technical teams and preserve infrastructure integrity. As networks evolve and become more complex, it is essential to continue research to adapt these methodologies to the sector's new challenges. The approach based on artificial neural networks (ANN) offers an effective method for fault localization in electrical networks but presents notable differences compared to classical techniques. Unlike wavelet-based methods and the Fourier transform, which provide clear physical interpretability, ANN excels in accuracy and adaptability to complex systems. Compared to impedance and current analysis methods, ANN proves to be more robust in evolving networks, although its dependence on training data may limit generalization. When compared to fuzzy logic models, ANN provides more precise classification but requires rigorous training. While ANN is a promising solution, its effectiveness could be enhanced when combined with hybrid approaches, improving both interpretability and model robustness. Continued research in this area could strengthen its integration into modern electrical systems and ensure better fault management.

## Acknowledgements

The authors gratefully acknowledge the Supelec and Matelek laboratories for their insightful discussions, technical assistance, access to computing resources, and valuable feedback throughout this work. Special thanks are also extended to Mr. YELEHANOU MOUKOKO Gotran Fildriche and Mr. NKOUMBOU Didier Medalvy Dieuville for their support and availability throughout this research.

## Conflicts of Interest

The authors declare no conflicts of interest regarding the publication of this paper.

## References

- [1] Gogom, M., Oko Ganongo, A., Apila, N. and Lilonga-Boyenga, D. (2020) Optimization of Power Transit through a Double-Term Line Term by the UPFC. *Science Journal of Energy Engineering*, **8**, 44-53. <https://doi.org/10.11648/j.sjee.20200804.11>
- [2] Hobeika, M.A. (1951) Les problèmes des réseaux électriques maillés et leur solution à l'aide des tables de calcul. PhD Thesis, ETH Zurich.
- [3] Ganongo, A.O., Gogom, M., Nianga-Apila, Obita, L.L.A. and Ganga, G. (2024) Optimisation of Lightning Current Discharge to the Ground in Electrical Networks: Introduction of the Proportionality Coefficient (K). *Electric Power Systems Research*, **231**, Article 110348. <https://doi.org/10.1016/j.epsr.2024.110348>
- [4] Alali, M.A.E. (2002) Contribution à l'Etude des Compensateurs Actifs des Réseaux Electriques Basse Tension: (Automatisation des systèmes de puissance électriques). PhD Thesis, Université Louis Pasteur (Strasbourg) (1971-2008).
- [5] Belatel, M. (2017) Compensation dans les réseaux électriques par un système facts de type statcom. In *5th International Conference of Renewable Energies CIER-17*, **30**, 37-42.
- [6] Boutaba, S. (2009) Amelioration de la stabilité d'un réseau par utilisation d'un SVC. PhD Thesis, Université Hassiba Ben Bouali Chlef, Faculte des Sciences et Sciences de l'Ingenieur.
- [7] Anderson, P.M. and Fouad, A.A. (2008) Power System Control and Stability. John Wiley & Sons.
- [8] Sauer, P.W. and Pai, M.A. (1998) Power System Dynamics and Stability, Prentice-hall. New Jersey.
- [9] Al Kazzaz, S.A.S., Ismaeel, I. and Mohammed, K.K. (2020) Fault Detection and Location of Power Transmission Lines Using Intelligent Distance Relay. *International Journal of Power Electronics and Drive Systems (IJPEDS)*, **11**, 726-734. <https://doi.org/10.11591/ijpeds.v11.i2.pp726-734>
- [10] Zimmerman, K. and Costello, D. (2006) Impedance-Based Fault Location Experience. *2006 IEEE Rural Electric Power Conference*, Albuquerque, 9-11 April 2006, 1-16. <https://doi.org/10.1109/repcon.2006.1649060>
- [11] Das, S., Santoso, S., Gaikwad, A. and Patel, M. (2014) Impedance-Based Fault Location in Transmission Networks: Theory and Application. *IEEE Access*, **2**, 537-557. <https://doi.org/10.1109/access.2014.2323353>
- [12] Al-Mohammed, A.H. and Abido, M.A. (2014) An Adaptive Fault Location Algorithm for Power System Networks Based on Synchrophasor Measurements. *Electric Power*

- Systems Research*, **108**, 153-163. <https://doi.org/10.1016/j.epsr.2013.10.013>
- [13] Spoor, D.J. and Zhu, J.G. (2006) Improved Single-Ended Traveling-Wave Fault-Location Algorithm Based on Experience with Conventional Substation Transducers. *IEEE Transactions on Power Delivery*, **21**, 1714-1720. <https://doi.org/10.1109/tpwrd.2006.878091>
- [14] Lin, S., He, Z.Y., Li, X.P. and Qian, Q.Q. (2012) Travelling Wave Time-Frequency Characteristic-Based Fault Location Method for Transmission Lines. *IET Generation, Transmission & Distribution*, **6**, 764-772. <https://doi.org/10.1049/iet-gtd.2011.0703>
- [15] Pouabe Eboule, P.S., Pretorius, J.H.C. and Mbuli, N. (2018) Artificial Neural Network Techniques Apply for Fault Detecting and Locating in Overhead Power Transmission Line. 2018 *Australasian Universities Power Engineering Conference (AUPEC)*, Auckland, 27-30 November 2018, 1-6. <https://doi.org/10.1109/aupec.2018.8757959>
- [16] Buragohain, M. and Mahanta, C. (2008) A Novel Approach for ANFIS Modelling Based on Full Factorial Design. *Applied Soft Computing*, **8**, 609-625. <https://doi.org/10.1016/j.asoc.2007.03.010>
- [17] Elnozahy, A., Sayed, K. and Bahyeldin, M. (2019) Artificial Neural Network Based Fault Classification and Location for Transmission Lines. 2019 *IEEE Conference on Power Electronics and Renewable Energy (CPERE)*, Aswan, 23-25 October 2019, 140-144. <https://doi.org/10.1109/cpere45374.2019.8980173>
- [18] Vasilic, S. and Kezunovic, M. (2002) An Improved Neural Network Algorithm for Classifying the Transmission Line Faults. 2002 *IEEE Power Engineering Society Winter Meeting. Conference Proceedings (Cat. No.02 CH37309)*, New York, 27-31 January 2002, 918-923. <https://doi.org/10.1109/pesw.2002.985139>
- [19] Mendoza, E.M.C. (2018) Méthodes de localisation et de détection de défauts d'arcs électriques séries dans un réseau électrique alternatif basse tension. Dissertation, Université de Lorraine.
- [20] Upadhyay, S., Kapoor, S.R. and Choudhary, R. (2018) Fault Classification and Detection in Transmission Lines Using Ann. 2018 *International Conference on Inventive Research in Computing Applications (ICIRCA)*, Coimbatore, 11-12 July 2018, 1029-1034. <https://doi.org/10.1109/icirca.2018.8597294>
- [21] De Metz-Noblat, Benoit, Dumas, F. and Poulain, C. (2005) Calculation of Short-Circuit Currents. Cahier Technique 158.

## Appendix

### Annexes A: Efficiency of RNA

**Table A1.** Efficiency of RNA for detection.

Type of fault	Desired output	RNA output	Mean detection error	Efficiency of RNA
A-G	1	0.99	0.01	99.99%
B-G	1	0.99	0.01	99.99%
C-G	1	0.99	0.01	99.99%
A-B-G	1	1.004	0.004	99.99%
A-C-G	1	1.006	0.006	99.99%
B-C-G	1	0.997	0.003	99.99%
A-B-C-G	1	0.999	0.001	99.99%
A-B	1	1	0	100%
A-C	1	1	0	100 %
B-C	1	0.991	0.009	99.99%
A-B-C	1	0.999	0.001	99.99%
No	0	0.0006	0.0006	99.99%
Total	.	.	.	99.99%

**Table A2.** Efficiency of RNA for classification.

Type of fault	Phases/ground (ABCG)	Desired output	RNA output	Error	Efficiency of RNA
*A-G	A	1	0.98	0.02	99.98%
	B	0	0.011	0.011	99.99%
	C	0	0.019	0.019	99.98%
	G	1	1.034	0.034	99.66%
*A-B-G	A	1	0.997	0.003	99.99%
	B	1	0.969	0.031	99.96%
	C	0	0.016	0.016	99.98%
	G	1	0.954	0.046	99.95 %
*A-B-C-G	A	1	0.988	0.02	99.8%
	B	1	0.982	0.08	99.2%
	C	1	1.017	0.017	99.97%
	G	1	0.89	0.11	99.98%
*A-B	A	1	1.014	0.014	99.98%
	B	1	0.99	0.01	99.99%
	C	0	0.003	0.003	99.99%
	G	0	0.04	0.04	99.96%

**Continued**

*A-B-C	A	1	0.98	0.02	99.98%
	B	1	0.98	0.02	99.98%
	C	1	1.017	0.017	99.98%
	G	0	0.44	0.44	99.56%
*No	A	0	0.021	0.021	99.97%
	B	0	0.025	0.025	99.98%
	C	0	0.026	0.026	99.98%
	G	0	0.09	0.09	99.91%
Total efficiency					99.96%

**Annexes B: Data on the Congolese Electricity Network**

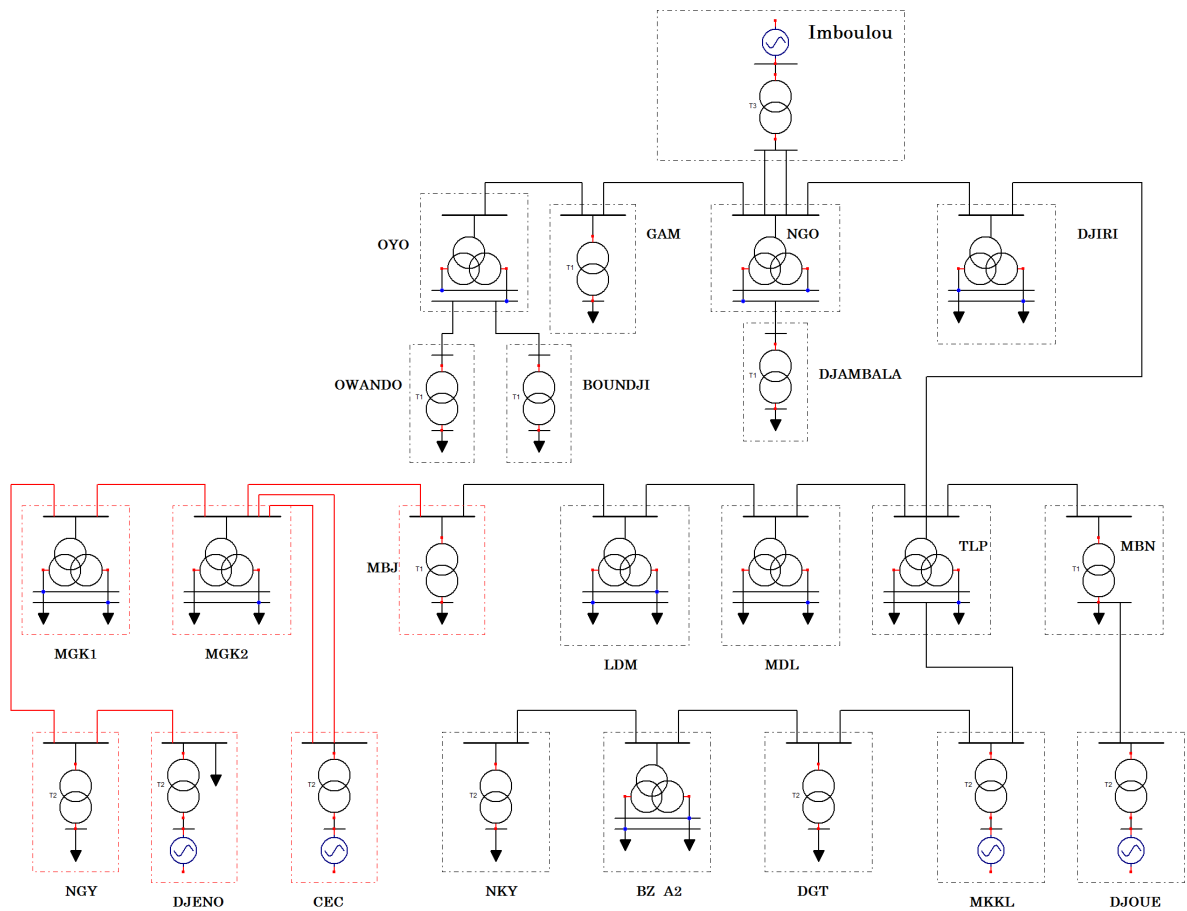


**Figure S1.** Congolese network.

**Table A3.** Transformer characteristics.

2*—	Voltage (KV)			Resistance			Inductance		
	Primary	Secondary	tertiary	Primary	Secondary	tertiary	Primary	Secondary	tertiary
T1	15.75	220	—	0.0014036	0.0011338	—	0.0641751	0.0641805	—
T2	220	30	—	0.0019708	0.0026074	—	0.089251	0.0892346	—
T3	220	30	20	0.0114286	0.0110204	0.010775	0.2368673	0.4141391	0.32883947
T4	220	30	20	0.0287467	0.01232	0.0257778	0.7327697	0.3140441	0.4793073
T5	220	30	—	0.016	0.0049383	—	0.4561195	0.2535075	—
T6	8.4	220	—	0.0118367	0.00209631	—	0.3426528	0.4557919	—

**Table A4.** Load characteristics.

	Load 1	Load 2	Load 3	Load 4	Load 5	Load 6	Load 7
P (MW)	84.15	42.5	26.7	22.95	53.54	50.4	12.3
Q (MVAR)	52	26.339	16.59	14.22	33.18	37.8	7.6

**Table A5.** Line characteristics.

Line	$R(\text{pu})$	$X(\text{pu})$	$b_0(\Omega^{-1})$
2-3 ( $\times 2$ )	0.001	0.014	3.619E-05
3-4	0.004	0.032	5.59391E-05
3-8	0.0005	0.003	0.0000005966
8-11	0.002	0.011	1.87458E-05
11-13	0.002	0.008	1.38129E-05

### Annexes C: Diagnostic System

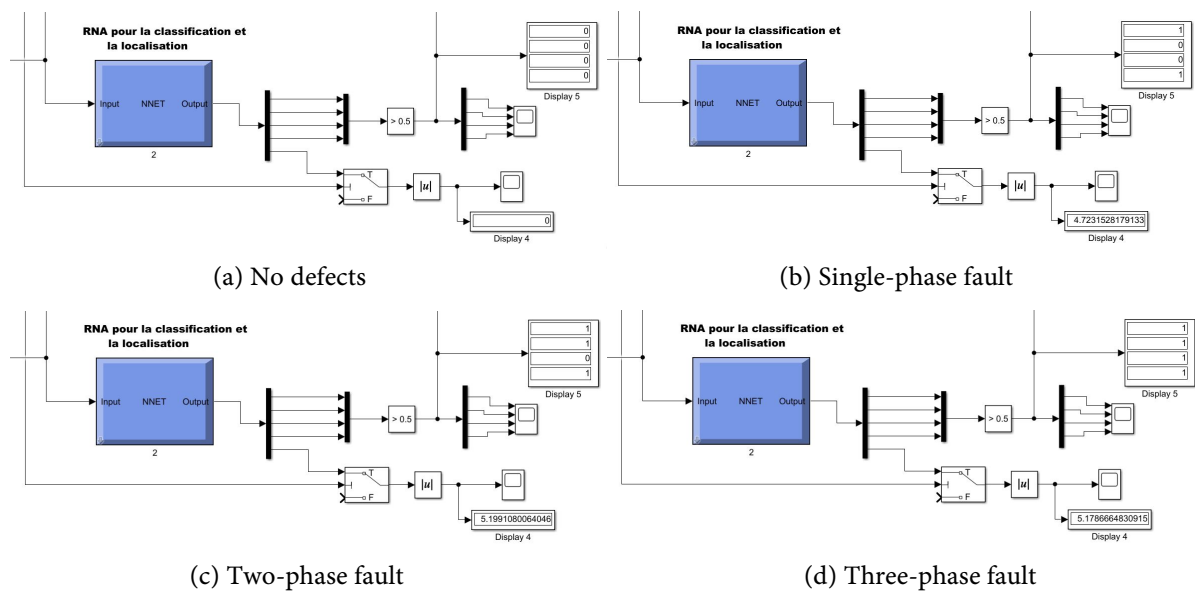


**Figure S2.** Architecture of the fault diagnosis system using neural networks.